www.sciencetranslationalmedicine.org/cgi/content/full/7/281/281ra45/DC1

Supplementary Materials for

Neuregulin stimulation of cardiomyocyte regeneration in mice and human myocardium reveals a therapeutic window

Brian D. Polizzotti, Balakrishnan Ganapathy, Stuart Walsh, Sangita Choudhury, Niyatie Ammanamanchi, David G. Bennett, Cristobal G. dos Remedios, Bernhard J. Haubner, Josef M. Penninger, Bernhard Kühn*

*Corresponding author. E-mail: bernhard.kuhn2@chp.edu

Published 1 April 2015, *Sci. Transl. Med.* **7**, 281ra45 (2015)
DOI: 10.1126/scitranslmed.aaa5171

This PDF file includes:

Table S2. Clinical information of patients with heart disease analyzed for Fig. 6C (H3P activity over age).
Table S3. Clinical information for normal hearts analyzed for Fig. 6C (H3P activity over age).
Table S4. Clinical information of patients with heart disease analyzed for Fig. 7D (rNRG1 stimulation).
Table S5. Clinical information of patients with heart disease analyzed for Fig. 8G (CFSE assay).
Table S6. Comparison of tissue response after cryoinjury in mice and myocardial disease in human infants (myocardial dysfunction, scar formation, and decreased cardiomyocyte cycling).
Table S7. Antibody manufacturers and dilutions.
Table S8. Image acquisition hardware and settings.
Table S9. Quantification of numeric data.
Table S10. Human primers for quantitative RT-PCR for calculation of fold change in expression levels.
Table S11. Mouse primers for quantitative PCR for calculation of fold change in expression levels.

Other Supplementary Material for this manuscript includes the following:
(available at www.sciencetranslationalmedicine.org/cgi/content/full/7/281/281ra45/DC1)

Fig.S3.data.pdf
Fig.S5.data.pdf
Fig.S6.data.pdf
Fig.S7.data.pdf
Fig.S8.data.pdf
Fig.S11.data.pdf
Table S1.GeneExpressionData.xlsx
Movie S1 (.mov format). BSA-treated mouse from early administration.
Movie S2 (.mov format). rNRG1-treated mouse from early administration.
Movie S3 (.mov format). BSA-treated mouse from late administration.
Movie S4 (.mov format). rNRG1-treated mouse from late administration.
Movie S5 (.mov format). 3D reconstructions show myocardial syncytium adjacent to the scar after early administration (64 dpi).

SUPPLEMENTARY MATERIALS AND METHODS

Considerations of rNRG1 concentration in vitro and rNRG1 dose in vivo.

We *(22)* and others *(30)* have shown that 100 ng/mL and 100 ng/g body weight of rNRG1 is sufficient to induce cardiomyocyte cycling in culture and adult mice. Our rationale for using 100 ng/mL in culture and 100 ng/g body weight in this study was to be able to reach concentrations that were previously shown to be able to stimulate cardiomyocyte cycling in vitro.

Quantification of myocardial function *in vivo* with echocardiography and cMRI. We performed sedated (1 - 1.5% isoflurane and 1 L/min oxygen) echocardiography using a Vevo 2100 device (VisualSonics) with a 30 MHz probe. M-mode recordings were obtained in the left parasternal short axis view and endocardial measurements were made on three consecutive cardiac cycles, repeated 9 times, for a total of 27 cardiac cycles per mouse for each data point. For cardiac cine-MRI, mice were anesthetized with 1-3% isoflurane in oxygen (1 L/min) and positioned prone in a purpose built cradle, containing a water-heated jacket to maintain body temperature. Respiration and ECG were monitored using a small-animal physiological monitoring system (SA Instruments, Inc.). The cradle was moved into a 9.4 T horizontal bore magnet (Bruker Biospin MRI, Billerica, MA, USA). A 40 mm inner-diameter quadrature volume coil (Bruker Biospin) was used for radio-frequency transmission and MR signal reception. For the late administration experiment, gadolinium was injected intraperitoneally at a dose of up to 0.3 millimoles/kg and imaged after 20 min. A stack of 6-7 contiguous 1 mm thick true short-axis cardiac-gated cine-FLASH bright-blood images (repetition time 20 ms; echo time 2.8 ms; 30 degree flip angle excitation pulse; field of view 2.56x2.56 cm; matrix size 256x256; voxel size 100x100x1000 μm; 5 frames per cardiac cycle) were acquired from base to apex. In the early administration experiment, short-axis images of the heart were acquired with the self-gating technique IntraGate (Bruker Biospin MRI, Billerica, MA, USA). The IntraGate technique is based on a fast low-angle shot (FLASH) gradient-echo pulse sequence with an extra gradient echo in which the respiration and cardiac motion information is embedded (4*6*). Using IntraGate, a stack of 6-7 contiguous 1 mm thick true short-axis self-gated cine-FLASH bright-blood images was acquired from apex to base. A separate 5 mm-thick navigator slice was carefully placed over the inflow tract of the ventricles in order to create the navigator gradient echo. A space of 0.5 mm was proscribed between the navigator slice and the last imaging slice. Voxel size in the short-axis slices acquired with IntraGate was 125x125x1,000 μm. The scan time per slice was approximately 3 minutes resulting in a total scan time of approximately 18-21 minutes per mouse.

Histology and quantitative morphometry. Mouse hearts were resected, washed in 50 mM KCl in PBS, weighed, and fixed in 3.7% (vol/vol) formaldehyde overnight. Hearts were then washed with PBS, equilibrated in a 30% (wt/vol) sucrose solution at 4^{o}C overnight, and mounted in tissue freezing medium (Triangle Biomedical Biosciences #TFM-5). Cryosections (18-20 μm thickness) were prepared with a Micron HM 550 (ThermoScientific) and re-fixed in 3.7% (vol/vol) formaldehyde for 15 min. For staining and analysis, sections were selected every 500 μm. For morphometry, 6-12 sections of each heart (~500 μm apart) were analyzed visually using either a Zeiss Axioplan 2 epifluorescent microscope with Plan-Neofluar 10x and 40x lens equipped with a Zeiss Axiocam CCD camera. To quantify scar, we analyzed 2x images of AFOG stained sections where fibrosis appears blue, which was digitally thresholded with Metamorph. The total scar volume (mm^3) was calculated by summing the scar area per tissue section multiplied by the distance between the selected sections (0.5 mm^3):

$$Total\ \ scar\ \ volume\ (mm^3) = \sum_{i=1}^{n} (Scar\ \ area_i \times 0.5mm)$$

where *n* is the total number of sections (6-12) and *i* is the first section starting at the apex. The scar size (% of myocardium) was determined by dividing the total scar volume by the total myocardial volume, determined by thresholding the red region (muscle):

$$Scar\ \ size\ (\%\ \ of\ \ myocardium) = \frac{\sum_{i=1}^{n} (Scar\ \ area_i \times 0.5mm}{\sum_{i=1}^{n} Muscle\ \ area_i \times 0.5mm} \times 100\%$$

Immunofluorescence microscopy and quantification of cell cycle activity. Cryosections (20 µm) were fixed in 3.7% (vol/vol) formaldehyde, permeabilized with 0.5% (vol/vol) NP-40 in PBS, and blocked with goat serum (20%, vol/vol, Sigma). To identify cardiomyocytes, we used primary antibodies against sarcomeric α-actinin (Sigma, 1:500). Karyokinesis was detected with an antibody against phosphorylated histone H3 (Upstate, 1:500). A monoclonal antibody against the Aurora-B kinase (Abcam, 1:1,000) was used to detect cytokinesis. The gap junctions were detected with a Connexin 43 antibody (Abcam, 1:200). Visualization was accomplished with secondary antibodies conjugated to either Alexa Fluor 488 or 594. Nuclei were visualized with 4', 6'-diamidino-phenylindole (DAPI, Invitrogen, 1:10,000) or Hoechst dye (1:1,000). Apoptosis was visualized with the ApopTag Red Kit (Millipore). Cardiomyocyte cell cycle activity was determined by manual counting of H3P positive CM nuclei. We analyzed 5 sections per heart (spaced approximately 600 µm apart). The area of each tissue section was determined using the method of point counts and the ratio of H3P CM nuclei per area of myocardium was calculated. Confocal images were obtained according to the information provided in **Supplemental Table S8**.

RNA-Seq sample preparation. Total RNA from mouse hearts was isolated using RNeasy Micro kit (Qiagen) using manufacturer's protocol. Each sample was assessed using Qubit 2.0 fluorometer and Agilent Bioanalyzer TapeStation 2200 for RNA quantity and quality. The mRNA molecules were purified using poly-T oligo attached magnetic beads and fragmented. The cleaved RNA fragments were reverse transcribed into first strand cDNA using reverse transcriptase and random primers. The cDNA library was constructed using the TruSeq Stranded mRNA kit (Illumina, San Diego, CA, USA).

The cDNA libraries were validated using KAPA Biosystems primer premix kit with Illumina-compatible DNA primers and Qubit 2.0 fluorometer. Quality was examined again using Agilent Bioanalyzer Tapestation 2200. The cDNA libraries were then pooled at a final concentration 1.8 pM. Sequencing was performed on NextSeq 500 instruments (Single-stranded, single-end indexed, 75 bp per read) at a depth of 35 x 10^6 per sample.

RNA-Seq analysis. Sequencing analysis was done using mRNA-Seq for differential expression in eukaryotes by Maverix Biomics (build 2.9). Raw sequencing reads (75bp, single read) were quality checked for potential sequencing issues and contaminants using FastQC. Adapter sequences, primers, Ns, and reads with quality score below 28 were trimmed using fastq-mcf of ea-utils and PRINSEQ. Reads with a remaining length of less than 20 bp after trimming were discarded. Single reads were mapped to the mouse genome (m10) using STAR in a strand specific manner. Read coverage on forward and reverse strands for genome browser visualization was computed using SAMtools, BEDtools, and UCSC Genome Browser utilities. Pairwise differential expression was calculated using Cuffdiff. Cufflinks was used to determine FPKM levels for each gene from the STAR

alignment and was used as input for Cuffdiff. All treatment groups were normalized to sham. Read counts were then normalized across all samples. Genes with significant change of expression were defined by an adjusted P-value < 0.05. Genes were sorted using log2 fold change as a sorting parameter. Functional annotation clustering was performed on David Bioinformatics Resource 6.7 online software.

Organotypic culture of human myocardium. Organotypic culture was performed as previously described with modifications (*38*). Briefly, specimens were transferred to ice-cold Ca^{2+} free Krebs-Ringer saline solution consisting of: 10 mM HEPES, 129 mM NaCl, 4.7 mM KCl, 1.2 mM KH_2PO_4, 1.2 mM $MgSO_4 \cdot 7H_2O$, 5 mM $NaHCO_3$, 5.5 mM glucose, 2 mg/ml bovine serum albumin (BSA), supplemented with 20 mM taurine, 2 mM l-carnitine, 5 mM creatine, and 30 mM 2,3-butanedione monoxime, pH 7.4. Medium 199 (M199, Gibco) or DMEM (Gibco) supplemented with 20 mM taurine, 2 mM L-carnitine, 5 mM creatine, 2 mg/ml BSA, 100 µU/ml penicillin and 100 µg/ml streptomycin, 1% heat inactivated fetal bovine serum (FBS, Gibco), or with 10^{-7} mM insulin (Roche). Prior to culture, samples were sliced 400-500 µm thick and cultured in laminin-coated 24-well plates (Costar) or 35-mm tissue culture dishes (Becton Dickinson). rNRG1 (100 ng/mL, R&D Systems, catalog#396-HB-050/CF) was added and organotypic cultures were maintained for 72 hours.

SUPPLEMENTARY RESULTS

Percentage of H3P cardiomyoyctes at 1dpi. To determine the percentage of H3P cardiomyocytes at 1dpi, we divided the number of H3P cardiomyocytes (identified by fluorescence microscopy) by the total number of cardiomyocytes in the sampled volume. The total number of cardiomyocytes in the sample volume was determined by multiplying the known sample volume by the cardiomyocyte density. To determine cardiomyocyte density, we first calculated the number of remaining cardiomyocytes 1 day after injury. Results from our TUNEL analysis showed that BSA treated animals lost an average of 29.29% of their myocardium whereas rNRG1 treated animals only lost 15.72% at 1dpi. Assuming that there are $1x10^6$ cardiomyocytes/ heart at 1 day of life, this leaves approximately 707,100 and 842,800 remaining cardiomyocytes for BSA and rNRG1 treated animals respectively (*16*). To calculate the cardiomyocyte density (cardiomyoytes/ mm^3) we divided the number of cardiomyocytes remaining by the volume of viable myocardium. This calculation suggests that the cardiomyocyte density was $3.01x10^5$ cardiomyocyte/mm^3 for both BSA (707,100 cardiomyocytes/ $2.35mm^3$) and rNRG1 (843,800 cardiomyocytes/ $2.78mm^3$) treated animals at 1dpi. This result gives 0.02% and 0.04% H3P positive cardiomyocytes for BSA and rNRG1 treated animals. It is important to note that this calculation represents a underestimate of the number of H3P cells. This is due to limitations inherent to imaging tissue sections 20 micrometers thick (*9)*.

Number of preserved cardiomyocytes. To determine if rNRG1 had a cardioprotective effect, we first examined the injury size following surgery. Morphometric analysis of hematoma size at 1 day post injury (dpi) shows no difference between BSA and rNRG1 treated animals (it is also worth noting that surgeries were preformed in a blinded fashion - i.e. the surgeon was unaware of the treatment group prior to surgery). We then calculated the number of remaining CMs 1 day after injury. Results from our TUNEL analysis showed that BSA treated animals lost an average of 29.29% of their myocardium whereas rNRG1 treated animals only lost 15.72% at 1dpi. These results suggest that rNRG1 protects against cell death following cryoinjury. Assuming that there are $1x10^6$ cardiomyocytes/heart at 1 day of life, this leaves approximately 707,100 and 842,800 remaining CMs for BSA and rNRG1 treated animals. In conclusion, rNRG1 treatment preserves approximately 136,000 cardiomyocytes.

Cardiomyocyte density and number at 34dpi. In order to determine if cardiomyocyte proliferation contributed to the regenerative process, we first counted the number of myocytes nuclei in the heart using unbiased stereology techniques. Using the optical dissector principle, we determined that the volume density of cardiomyocyte nuclei was $5.5x10^4$ and $6.8x10^4$ cardiomyocytes nuclei/mm^3 for BSA and rNRG1 treated animals. At 34 dpi, the percent of mono- and binucleated cardiomyocytes is roughly 20:80, which this equates to $3.1x10^4$ and $3.8x10^4$ cardiomyocytes/ mm^3. Using the myocardial volume, determined using the point counts method, we calculated the total number of cardiomyocytes/heart to be $1.79x10^6$ and $2.15x10^6$ cardiomyocytes at 34 dpi in BSA and rNRG-1-treated animals respectively. This equates to an increase of 355,556 cardiomyocytes in rNRG1 treated animals (or ~6940 cardiomyocytes/mm^3). Histological analysis showed no difference in heart weight/body weight, heart weight/ tibia length, or in cardiomyocytes size, suggesting that the observed increase in cardiomyocyte density is due to treatment with rNRG1.

Contribution of preserved cardiomyocytes to regeneration. To determine the contribution of cardioprotection to regeneration, we first determined the percent of H3P positive cardiomyocytes at 1dpi in rNRG1 treated animals (described above). This yields approximately 0.04% H3P CMs for rNRG1 treated animals. We know that cardioprotection rescued approximately 136,000 CMs. Assuming 0.04% of these cells proliferate according to published values (i.e. 1.8 hrs for karyokinesis, ref. *21*) for 34 days, yields 25,000 new CMs. It is important to note that this calculation is most likely an overestimate, as it assumes a linear proliferation rate for 34 days and assumes no binucleation events occur.

Contribution of cardiomyocyte proliferation to regeneration. To determine if endogenous cardiomyocyte proliferation could account for the increase in the number of cardiomyocytes (determined via stereology) we used our quantitative analysis of our H3P data to estimate the expected number of new cardiomyocytes using a linear regression model. H3P positive cardiomyocytes/mm^3 were quantified at 1, 10, and 34 days post injury for BSA and rNRG1 treated animals. The number of H3P positive cardiomyocytes/ mm^3 was plotted versus days post injury and a linear regression line was drawn (**Suppl. Fig. S1A**.). To determine the number of cardiomyocytes/mm^3 generated over the 34 day period, the graph was first segmented into the following days: 0-5 (segment 1), 5-6 (segment 2), 6-7 (segment 3), 7-8 (segment 4), 8-10 (segment 5), and 10-34 (segment 6) (Lines were drawn from the x-axis to the linear regression at the following dpi's: 5,6,7,8, and 10). The segmentation is needed to correct for the fraction of cardiomyocytes that binucleate. The area of each segment represents the total number of H3P positive cardiomyocytes/mm^3 for that time period. To calculate the area of each segment, a line was first extrapolated to the y-axis using the linear regression equation. This divides the segment into a triangle and a rectangular. An example is shown for segment 2 (i.e. from 5 dpi to 6 dpi, **Suppl. Fig. S1B**). The total area is calculated by summing the areas of the rectangle (A = length x width) and the triangle (A = 1/2 (base x height). The number of cardiomyocytes/mm^3 is then calculated assuming published proliferation rates (i.e. 1.8 hrs to complete karyokinesis) by multiplying the Area x Days in the segment x 24 hrs x 1/1.8hrs x % mononucleation (% mononucleation was determined from literature: 1-5 = 100%, 5-6 = 80%, 6-7 = 40%, 7-8 = 25%, > 8 = 10%). Summing the cardiomyocytes/mm^3 over all time segments yields the total cardiomyocytes/mm^3 over the 34-day period. If one assumes a 25% standard deviation (given the inherent error with the model i.e. continuous proliferation for 1.8hrs, etc) this give a range of 1.8-3.0x10^4 cardiomyocytes/mm^3 and 3.5-5.8x10^4 cardiomyocytes/mm^3 in the injury zone for BSA and rNRG1-treated animals, respectively. This value is within the range of cardiomyocytes/mm^3 in the whole determined by stereology techniques (3.1x10^4 cardiomyocytes/mm^3 vs 3.8x10^4 cardiomyocytes/mm^3). This result supports the observed increase cardiomyocyte density from 1 to 34 dpi and suggests rNRG1 stimulates endogenous CM proliferation.

Enhanced proliferation rate in rNRG1-treated animals. To estimate the increase in the absolute number of cardiomyocytes generated in rNRG-1 treated animals we plotted the difference in the absolute number of cardiomyocytes/mm^3 between BSA and rNRG1 treated animals (as calculated by H3P data). There is a dramatic and rapid increase in the number of cardiomyocyte/mm^3 from 1 to 10 dpi (slope = 3661 cardiomyocytes/mm^3/day, **Fig. 3K**). In other words, rNRG1 generates 36,661 additional cardiomyocytes/mm^3 in 10 days, relative to BSA treated animals, which accounts for approximately 78% of the total number of new cardiomyocytes generated. After day 10, the rate of cardiomyocyte proliferation decreases significantly (slope = 95.82 cardiomyocytes/mm^3/day), which would result in approximately 2299 new cardiomyocytes/mm^3 from day 10 to 34.

Relative contributions of cardiomyocyte proliferation from preserved and endogenous muscle to regeneration. As calculated above, we estimate that approximately 360,000 new cardiomyocytes are generated in rNRG1 treated animals. 136,000 cardiomyocytes are due to preservation, which means that 224,000 were produced from regeneration of endogenous muscle. 25,000 are due to proliferation of preserved muscle (See contribution of preserved cardiomyocytes to regeneration) or approximately 11% (25000/224,000 *100). Given that recent publications suggest that stem cells do not significantly contribute to regeneration in mice we attribute remaining ~89% to endogenous cardiomyocyte proliferation.

Relative contributions of preservation and cardiomyocyte proliferation to myocardial repair. Animals treated with rNRG1 from birth have an additional ~360,000 cardiomyocytes compared to BSA controls. rNRG1 protected 136,000 cardiomyocytes from death, therefore we estimate that preservation accounts for ~38% of the observed increase in cardiomyocyte content (136,000/360,000 = 0.38) at 34dpi. We estimate that approximately 25,000 cardiomyocytes are produced from the 136,000 cardiomyocytes preserved from rNRG1 treatment. This leaves 199,000 cardiomyocytes (360,000-136,000-25,000 = 199,000) formed by endogenous cardiomyocyte proliferation, and accounts for 62% ((199,000+25,000)/360,000) of the observed increase in cardiomyocyte number.

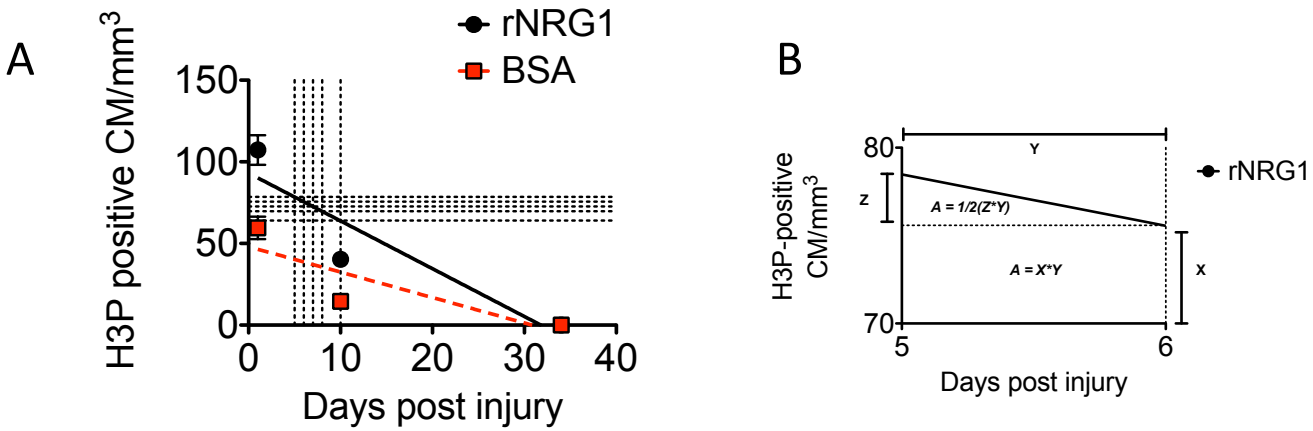

Suppl. Fig. S1. **Contribution of cardiomyocyte proliferation to regeneration**. **(A)** A graph of the number of H3P positive cardiomyocytes was plotted as a function of time (i.e. days post injury) and a linear regression analysis was performed. The linear regression was segmented into six different time points to account for the fraction of cardiomyocytes that binucleate during the first week of life. **(B)** To estimate the number of new cardiomyocytes generated the area of each segment was calculated using the equation: Area x Days in segment x 24hrs x rate of proliferation (1/1.8hrs) x % mononucleation (determined from literature). Summing the cardiomyocytes/mm^3 over all time segments yields the total number of cardiomyocytes/mm^3 over the 34-day period.

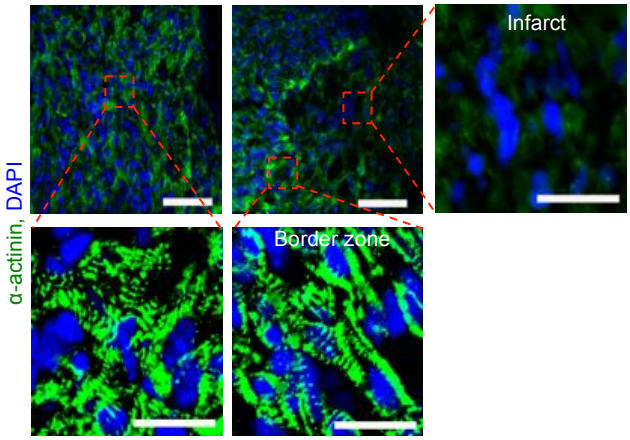

Fig. S2. **Cryoinjured hearts showed loss of sacromeric organization**. Tissue sections were stained with antibodies against α-actinin. The injured area has less sarcomeric signal and less striations. Scale bars: 100 μm (top) and 20 μm (bottom)

Fig. S3. **Characterization of myocardial repair following cryoinjury.**
[See fig.S3.data.pdf]
Hearts were sectioned in long axis and sections were selected every 500 μm and stained with Masson Trichrome Staining. Blue = scar, Red = muscle, 30 dpi.

BSA- 7765

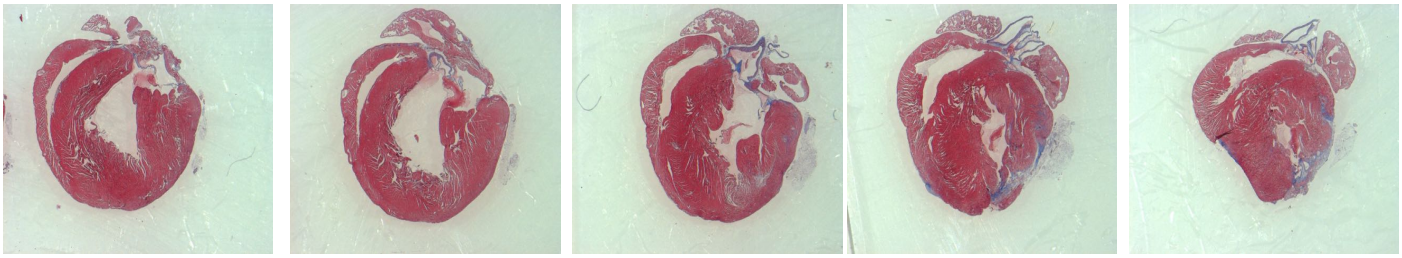

Fig. S4. **Transmural scar persists even after 7 months following cryoinjury.** Hearts were sectioned in long axis and sections were selected every 500 μm and stained with Masson Trichrome Staining. Blue = scar, Red = muscle, 210 dpi, early administration, BSA.

Fig. S5. Visualization of scar and quantification of cardiac function by MRI from early administration group. **[See fig.S5.data.pdf]**
Ten consecutive frames from one cardiac cycle were acquired from five to six different planes (spaced one millimeter apart) for each mouse analyzed. Animals were analyzed at 34 (a) or 64 dpi (b).

Fig. S6. Visualization of scar and quantification of cardiac function by MRI for late administration group. **[See fig.S6.data.pdf]**
Five consecutive frames from one cardiac cycle were acquired from six different planes (spaced one millimeter apart) for each mouse analyzed. Animals were analyzed at 34 (a) or 64 dpi (b).

Fig. S7. **Time course of myocardial repair following cryoinjury from early rNRG1 administration group. [See fig.S7.data.pdf]**
Tissue sections were selected every 500 μm and stained with acid-fuchsin orange-G. Blue = scar, Red = muscle, Orange = clot. 10, 30, and 60 dpi.

Fig. S8. **Time course of myocardial repair following cryoinjury from late rNRG1 administration group. [See fig.S8.data.pdf]**
Tissue sections were selected every 500 μm and stained with acid-fuchsin orange-G. Blue = scar, Red = muscle, Orange = clot. 10, 30, and 60 dpi.

APEX + 1 mm

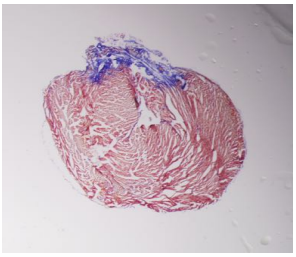

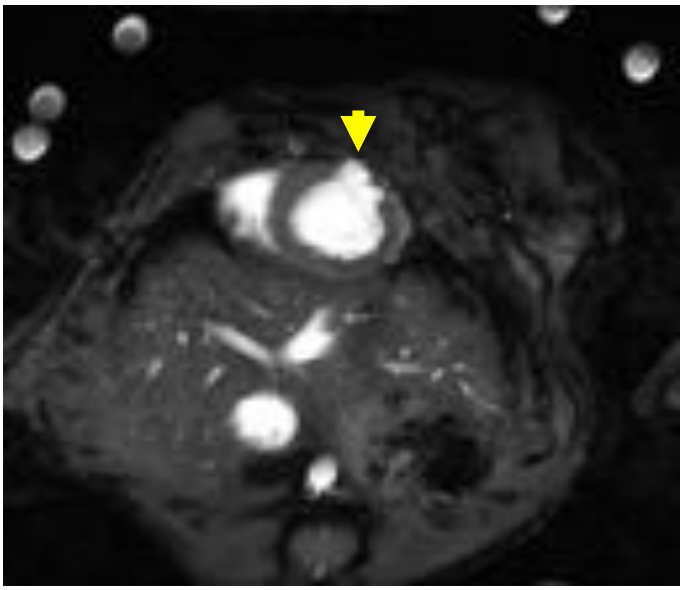

APEX + 2 mm

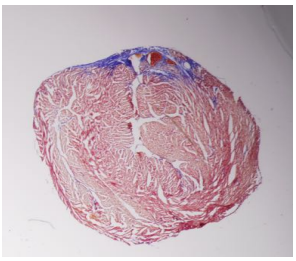

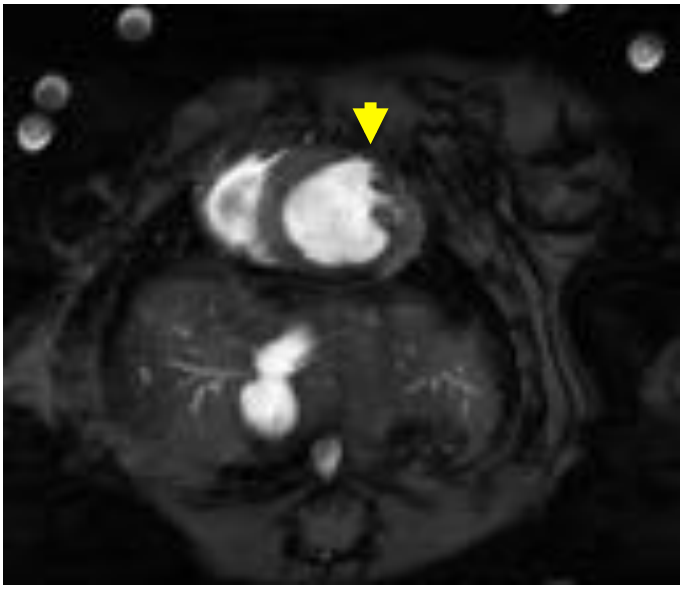

Fig. S9. **Failure to visualize transmural scars with late gadolinium enhancement due to low spatial resolution of cMRI in mice.** Mice underwent cryoinjury on day 1 of life (P1) and were treated with BSA from P5 (late administration). cMRI (with a 9.4 Tesla magnet) and heart resections were performed at 64 dpi. Hearts were sectioned in short axis and sections stained with acid fuchsin orange G (left panels). The position of the sections from apex is indicated on the left. cMRI images (right panels) corresponding to the level of AFOG sections do not show gadolinium enhancement in the region of transmural scars. Yellow arrows indicate region corresponding to scar. Blue = scar, Red = muscle.

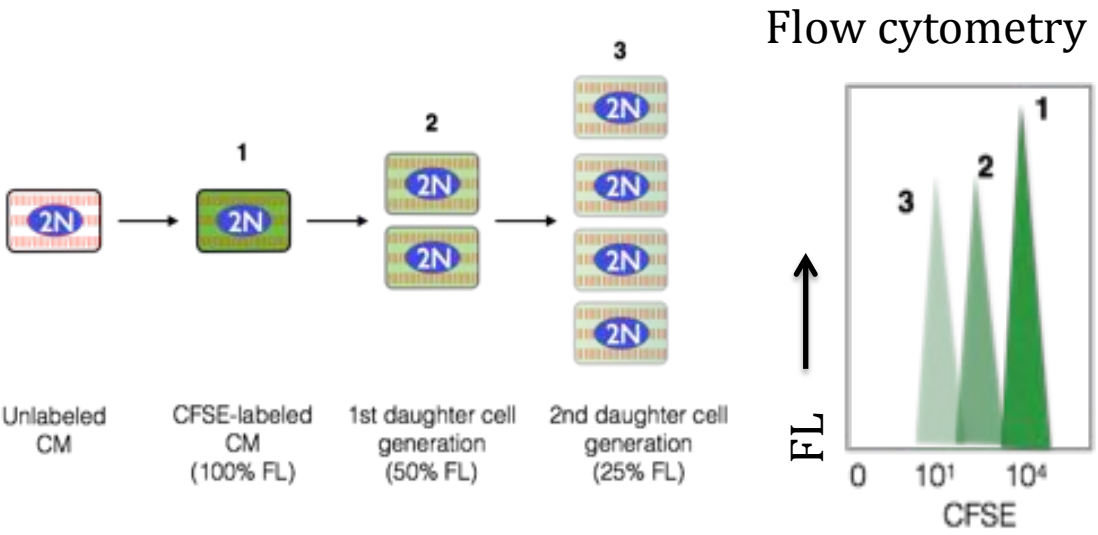

Fig. S10. Schematic representation illustrating the non-genetic labeling technique with CFSE. Organotypic cultures are treated with carboxyfluorescein succinimidyl ester (CFSE) which is taken up by the cell where it binds to proteins in the cytoplasm. Each division results in a decrease in the intensity of the CFSE dye by approximately 50% indicated by lighter hue of green. Quantification is accomplished by dissociation of the organotypic tissue sample followed by FACS analysis. FL, fluorescence intensity.

Fig. S11. rNRG1 stimulated cardiomyocyte proliferation in infants is age-dependent (2 months, 6 months, 1.5-5 year and 10 year old patients). [See fig.S11.data.pdf]

Human heart tissue samples were labeled with CFSE and cultured in organotypic culture in the presence of BSA/ rNRG1. Left column of panels shows scatter profiles of cardiomyocytes from 2 month-old patients (**Table S5**). Size and cellular complexity scatter profiles were used to enrich for the CM fraction, FSC/SSC high (**left panels**).The second column of panels shows how doublets were discriminated as a function of FSC-H and SSC-W. The third column of panels shows exclusion of dead cells by 7-AAD uptake. The right panels show assessment of rNRG1-stimulated proliferating myocardial cells (green outline), rNRG1 un-stimulated, but CFSE-loaded samples were used as controls (red outline) (**right panels**). CFSE-low populations were defined as populations having undergone cell-divisions (green gate), and the CFSE-high population withdrawn from the cell cycle, or not having undergone cytokinesis during the chase period.

Table S1. List of all differentially expressed genes between BSA and rNRG1 treatment groups, relative to sham mice (*P*<0.05). Mice underwent cryoinjury on day 1 of life (P1) and were treated with BSA or rNRG1 from day of birth (P0, early administration) till P12. Gene list shows 622 genes whose expression was significantly different (*P*<0.05, Student's t-test) in BSA- and rNRG1 treated mice relative to sham mice.
[See Table S1.GeneExpressionData.xlsx]

Table S2. Clinical information of patients with heart disease analyzed for Figure 6C (H3P activity over age).

Pt.no.	Age	Gender	Cardiac Disease	Site	Type of surgery	SpO_2 (%)	LVEF (%)
1	4D	M	VSD	RV	Repair	ND	54
2	7D	NA	NA	NA	Repair	NA	NA
3	2MO	NA	ToF/PS	RV	Repair	NA	NA
4	2MO	F	ToF/PS	RV	Repair	92 on O_2	61
6	3MO	M	ToF/PS	RV	Repair	95	64
7	3MO	M	ToF/PS	RV	Repair	95	61
8	4MO	M	ToF/PS	RV	Repair	95	67
9	4MO	NA	ToF/PS	RV	Repair	NA	NA
10	4MO	F	ToF/PS	RV	Repair	94	61
11	5MO	M	ToF/PS	RV	Repair	100	66
12	5MO	F	ToF/PS	RV	Repair	mid 90s on O_2	ND
13	6MO	NA	ToF/PS	RV	Repair	NA	NA
14	6MO	NA	ToF/PS	RV	Repair	NA	NA
15	7MO	NA	ToF/PS	RV	Repair	NA	NA
16	7MO	M	VSD	RV	Repair	96	61
17	8MO	F	DORV/PS	RV	Repair	73	42
18	16MO	M	VSD	RV	Repair	98	63
19	2Y	F	DCM	LV	LVAD	ND	28
20	16Y	M	DCM	LV	transplant	ND	30
21	17Y	M	DCM	LV	transplant	ND	26
22	19Y	M	ToF/PS	RV	PVR	96	NA
23	21Y	F	DCRV, VSD	RV	Repair	100	60
24	29Y	M	ToF/PS	RV	Repair	95	58

Myocardium was resected as part of standard care and collected in a de-identified fashion from the operating rooms at Boston Children's Hospital. Age, gender, cardiac diagnosis, type of surgery, oxygen saturation (SpO_2), and left ventricular ejection fraction (LVEF) at time of surgery are provided. Age is indicate in days (D), months (MO) and years (Y). Type of surgery: PVR, pulmonary valve replacement; LVAD, Left ventricle assist device. Patient no.4 had diGeorge syndrome; patient no.10 had Alagille syndrome. Abbreviations used: VSD, ventricular septal defect; ToF/PS, tetralogy of Fallot with pulmonary stenosis; DCRV, double-chambered right ventricle; DCM, dilated cardiomyopathy; DORV, double-outlet right ventricle; LV, left ventricle; RV, right ventricle; NA, not available; ND, not done.

Table S3. Clinical information for normal hearts analyzed for Figure 6C (H3P activity over age).

Pt.no.	Age (y)	Age	Gender	Site	Sample ID	Cause of death
1	0.06	3W	M	LV	6.012	hypoxic brain injury
2	0.17	2MO	F	RV	4.087	brain tumor
3	0.17	2MO	F	LV	4.087	brain tumor
4	1.2	14MO	F	RV	5.114	drowning
5	2	26MO	M	RV	7.05	drowning
6	4	4Y	M	RV	4.152	traumatic head injury
7	16	16Y	M	RV	6.072	hanged
8	19	19Y	F	RV	3.168	subarachnoid hemorrhage
9	23	23Y	M	RV	5.138	brain injury

Myocardium was provided by the University of Sydney (Sample ID corresponds to biobank ID). Cause of death was derived from the biobank database. Age is indicated in weeks (W), months (M), and years (Y). Abbreviations used: LV, left ventricle; RV, right ventricle.

Table S4. Clinical information of patients with heart disease analyzed for Figure 7D (rNRG1 stimulation).

Pt.no.	Age	Gender	Cardiac Disease	Site	Type of surgery	SpO_2 (%)	LVEF (%)
1	2MO	NA	ToF/PS	RV	Repair	NA	NA
2	2MO	F	ToF/PS	RV	Repair	92 on O_2	61
3	2MO	M	ToF/PS	RV	Repair	high 80's to mid 90	NA
4	3MO	M	ToF/PS	RV	Repair	95	64
5	3MO	M	ToF/PS	RV	Repair	95	61
6	3MO	M	ToF/PS	RV	Repair	95	56
7	5MO	M	ToF/PS	RV	Repair	100	66
8	5MO	F	ToF/PS	RV	Repair	mid 90s on O_2	NA
9	6MO	M	ToF/PS	RV	Repair	98	60
10	6MO	NA	ToF/PS	RV	Repair	NA	NA
11	6MO	NA	ToF/PS	RV	Repair	NA	NA
12	7MO	NA	ToF/PS	RV	Repair	NA	NA
13	15MO	M	ToF/PS	RV	Repair	80's on RA	55
14	17MO	M	ToF/PS	RV	Repair	100% finger oximetry	55
15	3Y	M	ToF/PS	RV	Repair	80	
16	4Y	NA	ToF/PS	RV	Repair	NA	NA
17	11Y	M	ToF/PS	RV	Repair	80	58
18	16Y	M	DCM	LV	Transplant	ND	26
19	29Y	M	ToF/PS	RV	Repair	95	58
20	66Y	M	ToF/PS	RV	Repair	96	43.5

Myocardium was resected as part of standard care and collected in a de-identified fashion from the operating rooms at Boston Children's Hospital. Age, gender, cardiac diagnosis, type of surgery, oxygen saturation (SpO_2), and left ventricular ejection fraction (LVEF) at time of surgery are provided. Age is indicated in days (D), months (MO) and years (Y). Abbreviations used: ToF/PS, tetralogy of Fallot with pulmonary stenosis; DCM, dilated cardiomyopathy; LV, left ventricle; RV, right ventricle; NA, not available; ND, not done.

Table S5. Clinical information of patients with heart disease analyzed for FIgure 8G (CFSE Assay).

Pt.no.	Age	Gender	Cardiac Disease	Site	Type of surgery	SpO_2 (%)	LVEF (%)
1	2MO	F	ToF/PS	RV	Repair	NA	62
2	2MO	F	ToF/PS	RV	Repair	92 on O_2	61
3	2MO	F	ToF/PS	RV	Repair	84-90	58
4	2MO	F	ToF/PS	RV	Repair	ully saturate	56
5	3MO	M	ToF/PS	RV	Repair	95	64
6	3MO	M	ToF/PS	RV	Repair	95	61
7	3MO	M	ToF/PS	RV	Repair	95	56
8	6MO	NA	ToF/PS	RV	Repair	NA	NA
9	6MO	M	ToF/PS	RV	Repair	98	60
10	6MO	M	ToF/PS	RV	Repair	> 98 on RA	NA
11	6MO	F	ToF/PS	RV	Repair	4/9/00	63
12	15MO	NA	VSD	RV	Repair	NA	NA
13	16MO	M	VSD	RV	Repair	98	63
14	3Y	M	ToF/PS	RV	Repair	80	NA
15	5Y	NA	ToF/PS	RV	Repair	NA	NA
16	10Y	M	HCM	LV	Myectomy	98	66

Myocardium was resected as part of standard care and collected in a de-identified fashion from the operating rooms at Boston Children's Hospital. Age, gender, cardiac diagnosis, type of surgery, oxygen saturation (SpO_2), and left ventricular ejection fraction (LVEF) at time of surgery are provided. Age is indicate in months (MO) and years (Y). Abbreviations used: ToF/PS, tetralogy of Fallot with pulmonary stenosis; VSD, ventricular septal deffect; HCM, hypertrophic cardiac myopathy; LV, left ventricle; RV, right ventricle; NA, Not available.

Table S6. Comparison of tissue response after cryoinjury in mice and myocardial disease in human infants (myocardial dysfunction, scar formation, decreased cardiomyocyte cycling).

	Cryoinjury	**Human infants with severe heart disease**	**Comments/ref.**
Myocardial dysfunction	Yes	Yes	(*36*)
Scar	Yes	Yes	(*36*)
Cardiomyocyte cycling	Decreased	Decreased	This manuscript

Table S7. Antibody manufacturers and dilutions.

Antibody/dye	Manufacturer	Dilution/concentration
Phosphorylated histone H3 at Ser10 (H3P)	Millipore	1:500
Sarcomeric α-actinin (α-actinin)	Sigma	1:500
Alexa- conjugated secondary antibodies	Invitrogen	1:200 to 1:500
Hoechst	Invitrogen	1:1,000
ApopTag Red In Situ Apoptosis Detection Kit	Millipore	Followed Manufacturer protocol
Pan-Cadherin	Sigma	1:500
Aurora B kinase	Abcam	1:250
DAPI	Sigma	1:1,000
Connexin 43	Sigma	1:200

Table S8. Image acquisition hardware and settings.

	Hardware	Software and settings
Fig 1A,B,F,G	Nikon SMZ 1000 stereoscope equipped with Olympus DP70 digital camera	1-3 sec exposure, Olympus DP Controller
Fig 1C,I	Olympus IX-81 spinning disk microscope with UPLAN FLN ×4, NA 0.13 and LUCPLFL ×60, NA 0.6 lens equipped with Hamamatsu EM CCD C9100. Zstacks: Range: 10mm; # Planes: 27: Step size: 0.3mm	20–500 msec exposure, Slidebook
Fig. 2H	Nikon SMZ 1000 stereoscope equipped with Olympus DP70 digital camera	1-3 sec exposure, Olympus DP Controller
Fig. 2L	9.4 T magnet (Bruker Biospin MRI)	Image J, Refer to Supplemental Materials and Methods for settings.
Fig. 2N (left panels)	Nikon SMZ 1000 stereoscope equipped with Olympus DP70 digital camera	1-3 sec exposure, Olympus DP Controller
Fig. 2N (middle panels)	Nikon A1Rsi Confocal 405nm, 488nm, 561nm, 640nm solid state lasers 10x Plan Apo Lambda 0.45NA	NIS-Elements Acquisition, Stitching and Analysis Software
Fig. 2N (right panels)	Nikon A1Rsi Confocal 405nm, 488nm, 561nm, 640nm solid state lasers 60x Plan Apo Lambda Oil 1.4NA NIS-Elements Acquisition and Analysis Software	NIS-Elements Acquisition and Analysis Software
Fig. 3A	Leica MZFLIII stereoscope equipped with Olympus DP70 digital camera	1-3 sec exposure, Olympus DP Controller
Fig. 3C,E,H	Olympus IX-81 spinning disk microscope with UPLAN FLN ×4, NA 0.13 and LUCPLFL ×60, NA 0.6 lens equipped with Hamamatsu EM CCD C9100. Zstacks: Range: 10mm; # Planes: 27: Step size:	20–500 msec exposure, Slidebook

	Hardware	Software and settings
	0.3mm	
Fig. 4B	Olympus IX-81 spinning disk microscope with UPLAN FLN ×4, NA 0.13 and LUCPLFL ×60, NA 0.6 lens equipped with	NIS-Elements Acquisition and Analysis Software
Fig. 6A	Olympus IX-81 spinning disk microscope with UPLAN FLN ×4, NA 0.13 and LUCPLFL ×60, NA 0.6 lens equipped with Hamamatsu EM CCD C9100.	20–500 msec exposure, Slidebook
Fig. 7A, C	Olympus IX-81 spinning disk microscope with UPLAN FLN ×4, NA 0.13 and LUCPLFL ×60, NA 0.6 lens equipped with Hamamatsu EM CCD C9100. Zstacks: Range: 20mm; # Planes: 10: Step size: 2mm	20–500 msec exposure, Slidebook
Fig. 7B	Nikon A1Rsi Confocal 405nm, 488nm, 561nm, 640nm solid state lasers 60x Plan Apo Lambda Oil 1.4NA NIS-Elements Acquisition and Analysis Software	NIS-Elements Acquisition and Analysis Software

Table S9. Quantification of numeric data.

Figure	Assay	Number of cardiomyocytes and/or hearts analyzed
Fig.1D	TUNEL Apoptosis	12 hearts analyzed, 3-5 sections/heart, 1 image/slide, 40x magnification
Fig. 1E	EF, echocardiography	40MHz probe, 153 animals analyzed
Fig. 1H	Fibrosis analysis	24 hearts analyzed, 10-15 sections/heart, 1 image/slide, 1x magnification
Fig. 1J	H3P positive cardiomyocytes	5 -10 sections/heart, 35 hearts analyzed
Fig. 2B,E	EF, echocardiography	40MHz probe, 159 animals analyzed
Fig. 2C,F	EF, cMRI	22 animals analyzed
Fig. 2D,G	Heart weight/tibia length	79 hearts weighed
Fig. 2I,J	Fibrosis analysis	69 hearts analyzed, 10-15 sections/heart, 1 image/slide, 2x magnification
Fig. 2K	Hearts with transmural scar	69 hearts analyzed, 10-15 sections/heart, 1 image/slide, 2x magnification
Fig. 2M	Left ventricular free wall thickening	22 hearts analysed, cMRI
Fig. 3B	Hematoma size	11 animals analyzed
Fig.3D	TUNEL Apoptosis	11 hearts analyzed, 3-5 sections/heart, 1 image/slide, 40x magnification
Fig. 3F,G	H3P positive cardiomyocytes	5 -10 sections/heart, 56 hearts analyzed
Fig. 3I	Aurora B positive cardiomyocytes	5 -10 sections/heart, 11 hearts analyzed

Figure	Assay	Number of cardiomyocytes and/or hearts analyzed
Fig. 3J,K	Stereology –CM nuclei density	11 hearts analyzed, 10-15 sections/heart, 5-7 image/slide, 60x magnification
Fig. 4C	H3P positive cardiomyocytes	11 hearts analysed, 3-5 sections/ heart, 1 image/ slide, 40x magnification
Fig. 5A	RNA-Seq heat map	15 hearts analysed (5 biological replicates were group)
Fig. 6C	H3P positive cardiomyocytes	33 human hearts analyzed
Fig. 7D	H3P positive cardiomyocytes	44 human hearts analyzed
Fig. 8G	Proliferating cardiomyocytes	16 human hearts analyzed

Table S10. **Human primers for qRT-PCR for calculation of fold change in expression levels**

Gene	Forward Primer	Reverse Primer
GAPDH	5'-ACCACAGTCCATGCCATCAC-3'	5'-TCCACCACCCTGTTGCTGT-3'
C-kit	5'-AGCAAATCCATCCCCACACC-'3	5'-GGCTTGAGCATCTTTACAGCGAC-3
cTNT	5′-GGCAGCGGAAGAGGATGCTGAA-3′	5′-GAGGCACCAAGTTGGGCATGAACGA-3′
DDR2	5'-TGTTCCTGCTGCTGCCTATCTT-3	5-AGGATAGCGGCATATAGCTGGAT-3
CD31	5′- ATTGCAGTGGTTATCATCGGAGTG-3′	5′- CTCGTTGTTGGAGTTCAGAAGTGG -3'
b-MHC	5-CAGTACATGCTGACAGACAGA-3'	5 –GCACATCAAAAGCGTTATCAG-3'
Ki-67	5'- CTTTGGGT-GCGACTTGACG-3'	5' - GTCGACCCCGCTCCTTTT-3
CCD1	5'- TTCATGTGGGCATTTCTTGCGAGC-3'	5'-CTGCCATTTGCTAGCAGTGTGACT-3'
CDKB1	5'-CAGTCAGACCAAAATACCTACTGGGT-3'	5'-ACACCAACCAGCTGCAGCATCTTCTT-3'
CDKA	5′-GCCATTAGTTTACCTGGACCCAGA-3′	5′-CACTGACATGGAAGACAGGAACCT-3'

Supplemental Table S11. **Mouse primers for qPCR for calculation of fold change in expression levels**

Gene	Forward Primer	Reverse Primer
ErbB4	5'- ACTATATGAAGATCGCTATGCC-3'	5'- CCACCATTTAGTATTTCGGTCAG-3'
HPRT	5′- TGATTAGCGATGATGAACCA-3′	5′- GCAAGTCTTTCAGTCCTGTC-3′

Captions for Supplemental Movies (S1-S5).

Supplemental Movie S1. BSA-treated mouse from early administration. Representative movie of cMRI frames at the level of papillary muscles at 64 dpi.

Supplemental Movie S2. rNRG1-treated mouse from early administration. Representative movie of cMRI frames at the level of papillary muscles at 64 dpi.

Supplemental Movie S3. BSA-treated mouse from late administration. Representative movie of cMRI frames at the level of papillary muscles at 64 dpi.

Supplemental Movie S4. rNRG1-treated mouse from late administration. Representative movie of cMRI frames at the level of papillary muscles at 64 dpi.

Supplemental Movie S5. 3D reconstructions show myocardial syncytium adjacent to the scar after early administration (64 dpi). Histologic heart sections (20 μm) through the injury site after early administration. Cardiac sarcomeres are depicted in red (α-actinin), gap junctions in green (Connexin 43), and nuclei in blue (Hoechst). Movies were generated from optical confocal sections 0.3 μm apart. A BSA-treated heart shows a scar (blue nuclei) lacking Connexin 43 positive cardiomyocytes (left movie, corresponding to Fig. 2N, top right panel). In contrast, an rNRG1 treated heart after early administration shows a scar with adjacent Connexin 43 cardiomyocytes (right movie, corresponding to Fig. 2N, bottom right panel).